

1 Ethanol exposure model in zebrafish causes phenotypic, behavioral and gene expression changes 2 that mimic Fetal Alcohol Spectrum Disorders in human birth cohorts

3 Elanur Yilmaz^{1,2,#}, Nastasia Nelson^{1,2,#}, Giuseppe Tosto^{1,2,3,*}, R. Colin Carter^{4,5,*}, Caghan Kizil^{1,2,3,*}

4

5 ¹ Department of Neurology, Columbia University Irving Medical Center, Columbia University, 710 W, 168th St, New
6 York, NY 10032, USA

7 ² The Taub Institute for Research on Alzheimer's Disease and the Aging Brain, Vagelos College of Physicians and
8 Surgeons, Columbia University Irving Medical Center, Columbia University, 650 W 168th St, New York, NY 10032,
9 USA

10 ³ The Gertrude H. Sergievsky Center, College of Physicians and Surgeons, Columbia University Irving Medical
11 Center, Columbia University, 630 W 168th St, New York, NY, USA

12 ⁴ Departments of Emergency Medicine and Pediatrics and the Institute of Human Nutrition, Columbia University,
13 Vagelos College of Physicians and Surgeons, Columbia University Irving Medical Center, New York, New York, USA

14 ⁵ Department of Human Biology, University of Cape Town Faculty of Health Sciences, Cape Town, South Africa

15

16 # These authors contributed equally

17 * These authors contributed equally

18

19 Correspondence: G.T. (gt2260@cumc.columbia.edu), R.C.C. (rcc2142@cumc.columbia.edu), C.K.

20 (ck2893@cumc.columbia.edu)

21

22 ABSTRACT

23 Fetal Alcohol Spectrum Disorders (FASD) represent a significant global health challenge, characterized
24 by physical and neurodevelopmental abnormalities in offspring resulting from prenatal alcohol exposure.
25 This study aims to utilize the zebrafish to examine the phenotypic, behavioral, and molecular changes
26 associated with embryonic ethanol exposure, providing a model for human FASD conditions. Our study
27 exposed zebrafish embryos to 0.5% ethanol during a critical developmental window (2-24 hours post-
28 fertilization) and documented significant craniofacial and cardiac deformities, which recapitulate what has
29 been observed in human FASD in humans. Notably, exposed zebrafish exhibited reduced skull and eye
30 sizes, thickened jaw size, and enlarged heart chambers. We found reduced burst swim distance following
31 a touch stimulus, a novel behavioral assessment of potential deficits in sensory processing such as
32 processing speed and/or stress/startle response, both of which are affected in human FASD. Whole-
33 organism gene expression was found to be altered by ethanol for orthologs of four of five inflammation-
34 related genes for which placental expression was previously found to be altered in response to alcohol in
35 human placentas (*SERPINE1*, *CRHB*, *BCL2L1*, *PSMB4*, *PTGS2A*). We conclude that the zebrafish model
36 effectively mimics several FASD phenotypes observed in humans, confirming gene expression changes
37 we have previously documented in a human observational study and providing a valuable platform for
38 exploring the underlying mechanisms of alcohol-induced embryonic alterations and for developing
39 diagnostic markers and therapeutic targets for early intervention.

40

41 KEYWORDS

42 Fetal Alcohol Spectrum Disorders, zebrafish, ethanol exposure, craniofacial abnormalities, behavioral
43 deficits, gene expression.

44

45 INTRODUCTION

46 Fetal alcohol spectrum disorders (FASD) are one of the foremost preventable causes of
47 neurodevelopmental disabilities worldwide. Prevalence estimates range from 1-5% in the US and Western
48 Europe (May et al., 2009) to 13.6-30.6% of school-aged children in endemic communities in South Africa
49 (May et al., 2021). FASD manifest a broad range of cognitive and behavioral deficits and growth restriction,
50 and teratogenic effects of alcohol have been reported in every organ system (Carter et al., 2016a; Carter
51 et al., 2012; Carter et al., 2016b; Hoyme et al., 2005; Jacobson, 1998). Despite behavioral intervention
52 programs and extensive prevention efforts (ACOG, 2011), ~18% of US women continue to drink during
53 pregnancy, with 6.6% reporting binge-drinking episodes (SAMHSA, 2010). Postnatal treatment programs
54 to improve cognitive abilities in children with FASD are limited by difficulties in identifying which children to
55 target. While fetal alcohol syndrome (FAS) is characterized by specific facial dysmorphology and growth
56 restriction (Hoyme et al., 2016; Hoyme et al., 2005), children with the most prevalent form of FASD, alcohol-
57 related neurodevelopmental disorder (ARND), are difficult to identify because they lack the characteristic
58 facial dysmorphology and are thus often identified later in life when early intervention approaches are less
59 effective. Yet these children still have cognitive impairments as severe as those with FAS. Thus, improved
60 diagnostic tools are needed, such as more fully characterized behavioral phenotypes and molecular
61 biomarkers of effect, e.g., gene expression profiles detectable at early life stages that identify children with
62 teratogenic effects of alcohol exposure. In prospective longitudinal birth cohorts in Cape Town, South
63 Africa, we helped to characterize the evolution of characteristic FASD dysmorphology across childhood
64 and adolescence (Jacobson et al., 2021), fetal alcohol-related neurobehavioral deficits (Carter et al., 2022;
65 du Plessis et al., 2015; Fan et al., 2016; Jacobson et al., 2011), including slower processing speed, and
66 alcohol exposure-related alterations in -placental expression of genes related to growth, inflammation, and
67 neurobehavior (Carter et al., 2018; Deysenroth et al., 2024; Masehi-Lano et al., 2023; Williams et al.,
68 2023).

69 As these and other FASD studies in humans are observational, animal models are needed to validate and
70 functionally characterize such findings. Zebrafish serve as a unique vertebrate experimental model system,
71 as they have unusually high morphological and genomic conservation with humans and experimental
72 mutability of embryogenesis and development that is mostly found in invertebrate animal models, such
73 as *C. elegans* or *D. melanogaster* (Adhish and Manjubala, 2023; Burgess and Burton, 2023). Furthermore,
74 the zebrafish genome and developmental transcriptome are well-characterized, with known timing of gene
75 expression patterns/profile and a well-described transition from expression of maternal genes in the egg
76 to embryonic genes in the maternal-zygotic transition in early development (Burgess and Burton, 2023;
77 White et al., 2017). Thus, the timing of teratogenic insults and their effects can be identified in experimental
78 models. Accordingly, FASD zebrafish models have led to foundational contributions to understanding of
79 the pathophysiological underpinnings of the teratogenic effects of alcohol. Zebrafish models have robustly
80 replicated structural effects of ethanol exposure on craniofacial, ocular, brain, and cardiac embryologic
81 development and have helped to elucidate genetic and molecular underpinnings of these effects (Adhish
82 and Manjubala, 2023; Fernandes and Lovely, 2021). Zebrafish models have also helped to characterize
83 alcohol-related behavioral deficits in social behavior, learning and memory, and anxiety phenotypic
84 outcomes (Adhish and Manjubala, 2023; Fernandes and Lovely, 2021).

85 In our FASD zebrafish model, we sought to replicate findings from our longitudinal human birth cohorts,
86 focusing on alcohol-related effects on craniofacial development, processing speed, and gene expression.
87 Such replication would validate the findings from our observational studies and establish readouts in FASD
88 zebrafish model that can be used in future experiments to identify genetic and molecular mechanisms
89 underlying these teratogenic effects of alcohol and potentially test therapeutic/preventive treatments
90 tailored to such mechanisms.

91

92 RESULTS

93 We implemented a zebrafish model to investigate the effects of embryonic ethanol exposure, aiming to
94 replicate and expand upon findings from human longitudinal birth cohorts that documented craniofacial
95 development alterations, processing speed deficits, and inflammation-related gene expression changes
96 due to prenatal alcohol exposure. We subjected zebrafish embryos to 0.5% ethanol exposure from 2 to 24
97 hours post-fertilization and conducted touch evoked response assay at three days post-fertilization (**Figure**
98 **1A**). Morphological measurements were done on day 4.5 to evaluate the overall body plan properly.

99 Phenotypic changes with alcohol exposure

L00 After ethanol exposure in zebrafish, we found significant craniofacial and cardiac abnormalities in the
L01 ethanol-exposed group (FASD) compared to controls (**Figure 1B, 1C**). In the sagittal plane, skull size was
L02 reduced in ethanol treated animals when compared to control animals [1.7 vs. 3.2 mm², $t(18)=3.743$,
L03 $p=0.0015$]. Eye size was similarly reduced (6.7 vs. 8.7 mm², $t(18)=3.807$, $p=0.0013$). To examine potential
L04 alterations in cranio-facial cartilage development, we performed Alcian blue staining in control and 0.5%
L05 EtOH-treated animals (**Figure 2A**) and observed significant alterations in jaw formation (**Figure 2B**).
L06 Ethanol treatment led to reduced distance between Meckel's cartilage (MK) and ceratohyal cartilage (CH)
L07 [101.81 μm vs. 85.29 μm, $t(53)=3.57$, $p=7.75E-04$], reduced length of MK [1,376.95 μm vs. 973.61 μm,
L08 $t(48)=6.229$, $p=1.2E-07$], and reduced dorsoventral cartilage thickness [172.71 μm vs. 106.50 μm,
L09 $t(24)=4.497$, $p=1.49E-04$]. The angle between CH formations was not altered [85.65 vs. 83.61 degrees,
L10 $t(53)=0.919$, $p=0.3622$]. This constellation of findings indicates disrupted chondrogenesis and growth
L11 patterns of the craniofacial skeleton consistent with facial hypoplasia. Ethanol treatment was also
L12 associated with an enlarged heart chamber (**Figure 1C**; 10.2 vs. 4.8 mm² in sagittal section, $t(26)=3.340$,
L13 $p=0.0025$).

L14 Alterations in behavioral and locomotor functions after alcohol exposure

L15 To determine whether alcohol exposure alters response to a stressful stimulus and the locomotor activity,
L16 we performed needle tail touch stimulus at 3 days after fertilization, in which a needle touches the tail of
L17 the animal causing a normative flight response (**Figure 3A, B**). The distance swum and the speed at which
L18 swimming occurs are both recorded. The burst swim response following a touch stimulus - a primitive reflex
L19 that is largely conserved across many species, including zebrafish and human - is a critical measure for
L20 the rapid escape behavior that relies on the proper processing of the environmental cue in the spinal cord
L21 and brain (Koutsikou et al., 2018). We found that ethanol-treated zebrafish displayed a decreased burst
L22 swim distance in response to a needle touch stimulus when compared to control animals (9.4 vs. 14.3 mm,
L23 $t(10)=2.370$, $p=0.0393$), indicating a diminished response to this stressful stimulus (**Figure 3C**). By
L24 contrast, swimming speed was unchanged (125.0 vs. 152.1 mm/second, $t(10)=-0.73$, $p=0.483$) (**Figure**
L25 **3C**).

L26 Gene expression changes in alcohol-exposed zebrafish

L27 We also examined whole-organism gene expression across a range of ethanol exposures for *serpine1*,
L28 *crhb*, *bcl2l1*, *psmb4*, and *ptgs2a*, zebrafish orthologs of inflammation-related genes found to be
L29 differentially expressed upon alcohol exposure in placenta samples in our human birth cohort (Deysenroth
L30 et al., 2024; Williams et al., 2023). Recapitulating our human placental findings, ethanol treatment was
L31 related to altered expression of four genes (**Figure 4**). For *serpine1*, a positive linear dose-response
L32 pattern was seen from ethanol concentrations of 0.5%, the concentration that most closely approximates
L33 human blood alcohol levels associated with FASD, and higher. For *crhb*, a negative linear dose-response
L34 pattern was seen from ethanol concentrations of 1% and higher. For *bcl2l1* and *psmb4*, gene expression
L35 was lower among animals with the highest exposure (2%) compared with unexposed control animals. Only
L36 *ptgs2a* showed no differential expression in response to staggered alcohol doses.

L37

L38 DISCUSSION

L39 In our FASD zebrafish model, we demonstrated the effects of embryologic ethanol exposure on craniofacial
L40 development, behavioral response to a needle touch stimulus, and expression of genes with roles in
L41 neuroinflammation, a key mechanism underlying ethanol-induced brain damage. These findings are
L42 consistent with prior findings in human studies (Carter *et al.*, 2018; Carter *et al.*, 2022; Deyssenroth *et al.*,
L43 2024; du Plessis *et al.*, 2015; Fan *et al.*, 2016; Jacobson *et al.*, 2021; Jacobson *et al.*, 2011; Masehi-Lano
L44 *et al.*, 2023; Williams *et al.*, 2023) and establish an experimental model for future examination of genetic
L45 and molecular pathways underlying the effects of alcohol on these outcomes.

L46 The ethanol-induced embryologic structural changes we demonstrated validate our FASD zebrafish model
L47 and experimental paradigm, as such anomalies parallel previous zebrafish models and well-documented
L48 phenotypes associated with FASD in humans, including reduced head circumference and characteristic
L49 ocular dysmorphologies (Cadena *et al.*, 2020; Fernandes *et al.*, 2014; Sarmah *et al.*, 2016; Sidik *et al.*,
L50 2021). As expected from prior FAD zebrafish models (Alsakran and Kudoh, 2021; Fernandes and Lovely,
L51 2021), embryologic ethanol exposure from 2-24 hours post-fertilization led to reductions in skull and eye
L52 size, cranial hypoplasia, and enlargement of the heart chamber. Embryonic reductions in skull size are the
L53 result of smaller brain size, and the human analogue, reduced head circumference, is one of the key
L54 diagnostic criteria for FAS and partial FAS (Hoyme *et al.*, 2016; Hoyme *et al.*, 2005; Jacobson *et al.*, 2021).
L55 Previous zebrafish experiments have demonstrated ocular defects in ethanol-exposed zebrafish, including
L56 reduced eye size, as we have shown here (Dlugos and Rabin, 2007). In humans, fetal alcohol effects on
L57 the visual system are well-documented (Carter *et al.*, 2005; Stromland, 1987), and ocular dysmorphic
L58 features are characteristic of FASD dysmorphology, including inner- and outer-canthal distances,
L59 interpupillary distance, and, most notably, palpebral fissure length, i.e., the measure of the length of the
L60 eye opening (Gomez *et al.*, 2020; Jacobson *et al.*, 2021). Indeed, reduced palpebral fissure length is one
L61 of the three hallmark dysmorphic features used in FASD diagnostic criteria (Hoyme *et al.*, 2016; Hoyme *et al.*
L62 *et al.*, 2005). Embryologically, reductions in palpebral fissure length are thought to be driven by reduced
L63 ocular size and alterations in forebrain development, consistent with our findings. Our finding of ethanol-
L64 associated facial hypoplasia has been previously shown in zebrafish models (Sidik *et al.*, 2021), and, in
L65 the midface, is well-characterized in humans (Muggli *et al.*, 2017; Suttie *et al.*, 2013; Suttie *et al.*, 2017).
L66 Lastly, although the cardiotoxic effects of prenatal alcohol exposure in humans are more variable and less
L67 well-characterized than craniofacial dysmorphology, our finding of ethanol-induced heart chamber
L68 enlargement is consistent with prior zebrafish models (Dlugos and Rabin, 2007).

L69 These morphological changes observed in our zebrafish model reflect disruptions in developmental
L70 processes that are critical for normal organogenesis. Ethanol exposure might be interfering with several
L71 key pathways. Alcohol inhibits the proliferation of neural crest cells and disrupt their migration patterns
L72 (Smith *et al.*, 2014). Neural crest cells are essential for the development of craniofacial structures and the
L73 heart (Achilleos and Trainor, 2012). Impaired migration and differentiation of these cells due to ethanol
L74 exposure could lead to the craniofacial abnormalities and cardiac defects we observed. Additionally,
L75 ethanol might affect the expression and function of genes critical for development. This includes genes
L76 involved in the growth and differentiation of cells in the craniofacial region and heart. It is known that ethanol
L77 metabolism produces reactive oxygen species (ROS), leading to oxidative stress which can damage cells
L78 and tissues, impairing normal development (Qin and Crews, 2012). This oxidative stress is particularly
L79 detrimental during the rapid growth and differentiation stages of early embryogenesis as it can induce
L80 apoptosis in developing tissues (Redza-Dutordoir and Averill-Bates, 2016). The correlation of the
L81 phenotypes in zebrafish to humans not only underscores the utility of the zebrafish model in mimicking
L82 human FASD phenotypes but also provides a controlled environment to further explore the specific
L83 mechanisms by which alcohol alters embryonic development.

L84 We also demonstrated ethanol-induced reductions in burst swim distance seen after a needle-touch
L85 stimulus to the animal's tail. This finding is particularly significant as it represents a novel behavioral
L86 assessment in the FASD zebrafish model. To our knowledge, no prior study has examined this outcome
L87 in an FASD zebrafish model. The observed deficit in burst swim distance may reflect diminished sensory
L88 processing, slower processing speed, diminished startle response, and/or gross locomotor deficits.
L89 Interestingly, despite these reductions in burst swim distance, our study did not find significant changes in

L90 gross locomotor function as indicated by swimming speed (**Figure 2C**). This suggests that the primary
L91 effect of ethanol exposure may be on the sensory and neural processing pathways rather than on the basic
L92 motor functions.

L93 The ability to respond to a needle touch with a rapid swimming motion also involves sensory processing
L94 (Abraira and Ginty, 2013), which is coordinated by multiple neural circuits, including sensory detection,
L95 signal processing in the nervous system, and motor execution. In a normative response, the sensory
L96 systems must detect the stimulus, the nervous system must process this information, and the motor
L97 systems must execute the escape response. Impairments in any part of this sensory integration pathway
L98 can result in a diminished response. The diminished burst swim response indicates that prenatal ethanol
L99 exposure could impair these critical neural pathways. This is consistent with human studies showing that
L100 individuals with FASD often have slower processing speed and impaired startle responses, which can
L101 affect their daily functioning and response to environmental stimuli. We and others have demonstrated
L102 prenatal alcohol exposure-associated processing speed deficits in human studies (Burden et al., 2009;
L103 Carter *et al.*, 2022; Fan et al., 2017; Jacobson, 1998; Jacobson et al., 1994; Willford et al., 2010), which
L104 may have pervasive functional relevance in activities of daily living and function in employment for affected
L105 individuals. The burst swim is part of the startle response, a fundamental survival mechanism. This
L106 response can also be influenced by the hypothalamic-pituitary-adrenal (HPA) axis. Animal models and
L107 human studies have demonstrated fetal alcohol-induced alterations in the hypothalamic-pituitary-adrenal
L108 (HPA) axis and stress-responses, with blunted behavioral and biochemical responses seen early in life
L109 and overactive responses and related mental health issues later in life (Fifer et al., 2009; Hellemans et al.,
L110 2010; Oberlander et al., 2010; Ruffaner-Hanson et al., 2022). Our findings underscore the utility value of
L111 using zebrafish as a model to study the specific neural and molecular mechanisms underlying these
L112 behavioral deficits. Future studies should focus on further characterizing the ethanol-induced changes in
L113 sensory processing and startle response pathways. Investigating the neural circuits and gene expression
L114 profiles involved in these behaviors could provide deeper insights into how prenatal alcohol exposure
L115 disrupts brain development and function. Moreover, understanding these mechanisms may open avenues
L116 for developing targeted therapeutic interventions to mitigate the effects of FASD on sensory and neural
L117 processing.

L118 A growing body of literature has implicated neuroinflammation in fetal alcohol-related brain damage (Kane
L119 and Drew, 2021). For example, in a rat model, prenatal alcohol exposure led to higher levels of cytokines
L120 and chemokines in the fetal brain and the placenta, higher cytokine/chemokine response to
L121 lipopolysaccharide stimulation in the adult offspring brain, and related memory impairments (Terasaki and
L122 Schwarz, 2017). Our findings of ethanol-induced alterations in *serpine1*, *crhb*, *bcl2l1*, and *psmb4* gene
L123 expression are consistent with our recent reports of alcohol-related alterations of these and other
L124 inflammation-related genes in alcohol exposed placenta samples from a human longitudinal birth cohort
L125 (Deyssenroth *et al.*, 2024; Williams *et al.*, 2023). These findings validate our prior findings in humans and
L126 identify pathways that can be explored for future studies of targeted therapeutics. In the current study, a
L127 positive dose-response relationship was seen between ethanol exposure and zebrafish *serpine1*
L128 expression. These findings are consistent with our finding of alcohol exposure-related increases in
L129 placental expression of the human analogue, *SERPINE1*, which encodes a member of the serine
L130 proteinase inhibitor (serpin) superfamily that plays roles in antiviral immunity and contributes to regulation
L131 of neuroinflammation (Pelisch et al., 2015; Pu et al., 2022; Wang et al., 2021). In our zebrafish model,
L132 ethanol was associated with decreased *crhb* expression. *crhb* in zebrafish and its analogue *CRH* in
L133 humans are key regulators of the hypothalamic-pituitary-adrenal (HPA) axis; disruptions in the HPA axis
L134 have been repeatedly demonstrated to play roles in FASD inflammation-related pathophysiology in both
L135 animals and humans (Ruffaner-Hanson *et al.*, 2022). Interestingly, while *crhb* expression was decreased
L136 in response to ethanol in our zebrafish model, *CRH* was increased in our human placenta study. This
L137 difference may be due to differences between species (e.g., zebrafish do not have placentas). Notably,
L138 prior FASD zebrafish models have shown both up- and down-regulation of *crhb* in response to
L139 developmental ethanol exposure, depending on the developmental timing of the exposure and the age at
L140 which *crhb* expression was measured (Du et al., 2020). The ethanol-induced reductions in *bcl2l1* seen in
L141 our zebrafish model match our finding in human placentas and prior work demonstrating decreased hepatic
L142 expression of *BCL2L1* in ethanol-exposed rats (French et al., 2005) and decreased expression in an

ethanol-treated mouse hippocampal cell line (HT22) (Song et al., 2014). The human analogue *BCL2L1* is a regulator of apoptosis via reactive oxygen species production and cytochrome C release in mitochondria. Its isoform Bcl-X(L) also regulates presynaptic activity, neurotransmitter release/recovery, as well as synaptic vesicle formation and endocytic vesicle retrieval in the hippocampus. In an immune function role, it may impair NLRP1-inflammasome activation (Bruey et al., 2007), which is notable since *bcl2l1* was down-regulated in ethanol exposed animals in the current study. *psmb4* expression was decreased in response to ethanol exposure, consistent with our finding in human placentas of alcohol-related reductions in expression of *PSMB4*, which encodes a proteasome subunit important for the immunoproteasome that facilitates non-lysosomal, ubiquitin-independent peptide cleavage necessary for MHC class I-presented antigenic peptides (Verhoeven et al., 2022). Although the mean fold change expression levels for *ptgs2* were higher in the 1% and 2% ethanol treatment groups than for the lower concentration groups, these differences were not statistically significant. *PTGS2* encodes the inducible form of prostaglandin-endoperoxide synthase, a.k.a., cyclooxygenase, a key enzyme in prostaglandin synthesis that plays roles in the creation of resolvins (resolution phase interaction products) during inflammation (Serhan et al., 2002) and in neuronal secretion of specialized preresolving mediators (SPMs) that regulate phagocytic microglia. The mouse analogue, *Ptgs2*, has been shown to play key roles in neuroinflammation regulation in cerebral ischemia (Jiang et al., 2023) and traumatic brain injury (Graber et al., 2015).

While our model offers substantial insights, it has limitations. The controlled environment of our study may not fully encapsulate the complexity of alcohol metabolism in a pregnant human, where varying factors such as genetics, overall health, nutritional status, and additional substance use can significantly affect the teratogenic outcomes. Our study did not examine potential cumulative effects of repeated or prolonged exposure to ethanol, as might be more typical in human scenarios of alcohol use during pregnancy. Future studies could look to model different patterns of exposure to better replicate the range of exposure scenarios seen in human populations. Early developmental models do not answer the long-term effects of early alcohol exposure. Longitudinal studies within our zebrafish model could provide further insights into how early alcohol exposure influences adult phenotypes, particularly in neurobehavioral contexts.

Overall, our findings demonstrate that the zebrafish FASD model effectively replicates and extends critical aspects of human FASD, including morphological changes, behavioral deficits, and molecular alterations. This model not only helps in understanding the pathophysiological basis of FASD but also provides a viable platform for testing potential interventions and studying the underlying molecular mechanisms in a controlled environment. We replicated fetal alcohol-related effects on craniofacial and heart development, behavior, and gene expression seen in prospective longitudinal birth cohorts. Furthermore, we established a new FASD zebrafish model, which includes a novel alcohol-related needle-touch behavioral deficit, consistent with processing speed and/or stress-response changes in human studies. Our FASD zebrafish model may be used in future work to examine how specific genetic factors, identified in human studies, influence fetal development in the setting of ethanol exposure and could uncover critical periods of vulnerability to ethanol, thus enhancing our understanding of FASD susceptibility. Functional characterization of genetic variants associated with FASD could elucidate the molecular mechanisms driving this disorder. This could involve assessing how these variants impact gene expression, protein function, and cellular pathways. For example, employing CRISPR/Cas9 technology to edit genes implicated in FASD within this model could validate the roles of specific genes and uncover potential therapeutic targets.

285

286 **MATERIALS AND METHODS**

287 **Zebrafish husbandry**

288 Adult animals were maintained under temperature and humidity-controlled environment of Columbia
289 University Medical Center on a 14/10-h light/dark cycle, with ad libitum access to food and water in
290 compliance with the protocols approved by the Institutional Animal Care and Use Committee of Columbia
291 University (IACUC). All zebrafish experiments were performed in larval stages (up to day 5) in accordance
292 with the applicable regulations by the IACUC. Adult male/female zebrafish with a 3:3 ratio was isolated in
293 slope breeding tank with a divider. The next morning, dividers were removed, and the eggs were collected

194 30 minutes after crossing. The eggs were collected and incubated in 28.5°C incubator. 2 hours later
195 fertilized eggs with normal developing stage were randomly selected and distributed to the experimental
196 groups, while unfertilized eggs with abnormal development and/or malformations were discarded. The
197 survival rate of animals in the control group at day 1 was $\geq 95\%$ and the hatching rate was 100% at day 3.

198 **Ethanol preparation and treatment**

199 Absolute ethanol (Lot: 222257, CAS # 64-17-5, Fisher Bioreagents) was used to prepare 0.25%, 0.5%,
200 1%, 2% ethanol concentrations. EtOH solution prepared freshly before the experiment and added to the
201 embryo medium. We followed the methodology of FASD models as described before (Cadena *et al.*, 2020;
202 Sarmah *et al.*, 2016). In short, the healthy embryos were raised in embryo medium with methylene blue
203 until 2 hour-post-fertilization (hpf). Developmental stages were defined as described (Kimmel *et al.*, 1995;
204 Kimmel *et al.*, 1988). At 2 hpf, equal number of embryos were transferred to the embryo medium without
205 methylene blue (untreated, control group) and medium with related EtOH concentrations (0.25% (~50mM),
206 0.5% (~100mM), 1% (~200mM), 2% (~400mM) in Petri dishes by wrapping with Parafilm®. Following the
207 22 hours of exposure (at 24 hpf), all solutions were replaced with fresh embryo mediums with methylene
208 blue. All experimental groups were raised in 28.5°C incubator until the experiment.

209 **Behavioral measurements**

210 Embryos that are dead or have severe morphological defects ($\leq 9\%$ for all groups) were excluded from the
211 behavioral test. In the end we analyzed the touch evoked response in 6 embryos in each group. The larvae
212 were placed in a large petri dish under grid paper (0.50 cm per gridbox). A dissecting scope attached digital
213 camera (AmScope, SM-4T) was elevated 12 inches to enable a wider view of the larvae in the dish. One
214 larva at a time was transferred into the dish using a Pasteur pipette. After acclimation, the larvae were
215 prodded with a fine point syringe needle on the tail until an attempted to escape was prompted, and
216 swimming response were recorded.

217 **Video analysis**

218 The larvae videos were analyzed utilizing iMovie. The number of needle touches before an escape attempt
219 was recorded. The Start Time was considered the last needle touch before larva locomotion (or larva's
220 escape attempt). The End Time was the first stop made by the larva after the escape attempt. The distance
221 travelled was calculated by multiplying 0.50 cm by the number of grid boxes traveled. The rate of travel
222 was evaluated by subtracting the start time from the end time and dividing it by the distance travelled.
223 Additionally, we utilized iMovie's freeze frame and slow-motion features to accurately capture the above
224 perimeters and straight path criteria. The straight path variable was defined as the larva changing direction
225 after proceeding on a specific path.

226 **Alcian Blue staining**

227 Alcian blue staining was performed [as described in (Neuhauss *et al.*, 1996)] to 4 dpf zebrafish larvae of
228 control and 0.5% EtOH treated group to detect craniofacial cartilage morphology. Briefly, zebrafish larvae
229 were fixed in 4% PFA in PBS overnight in cold room. The rest of the steps were performed at room
230 temperature, and on the shaker. After fixation, larvae were washed three times with PBST, each washing
231 was for 5 min. Larvae then were dehydrated by using 50% ethanol for 15 min and stained overnight with
232 Alcian Blue (Sigma, Cat no: B8438). The next day, larvae were washed with PBST for 5 min and bleached
233 (30% H₂O₂ (Sigma, Cat no: H1009) and 2% KOH (Sigma, Cat no: 417661)) for 1 hour. After removing the
234 bleach solution, larvae were washed for 5 min with PBST and cleared with 25% Glycerol (Sigma, Cat no:
235 G5516) contains 0.25% KOH and stored in 50% Glycerol with 0.25% KOH until imaging with Zeiss
236 Discovery. V12 with AxioCam MRc and AxioVision LE64 software.

237

238 **Morphological analysis**

239 At day 4.5, control and 0.5% EtOH-treated experimental groups were analyzed by their craniofacial (eye
240 distance, eye and skull size, jaw position), cardiac (heart chamber size), and overall morphological
241 phenotypes (body length, spine deformation, tail deformation, yolk sac edema, swim bladder inflation). For
242 craniofacial cartilage analysis, distance between rostromedial regions of Meckel cartilage (MK) and

343 ceratohyal cartilage (CH) (on ventral views), length of the MK (on ventral images), angle between lateral
344 CH cartilages (on ventral images), and the cartilage thickness below the lens (lateral images) were
345 measured using ImageJ software 2.1.0/v1.53.c.

346 **Quantitative real-time PCR**

347 We examined zebrafish orthologs for 5 candidate inflammation-related genes found to be differentially
348 expressed based on alcohol exposure (control (n=11), 0.25% (n=11), 0.5% (n=12), 1% (n=12) and 2%
349 (n=12)) in human placentas in our prospective birth cohort (Deysenroth *et al.*, 2024; Williams *et al.*, 2023).
350 RNA isolation of pooled embryos of each group was performed by using TRIzol[®] Reagent (Invitrogen,
351 15596026) and Direct-zol RNA Microprep Kit (Zymo Research, R2060) according to the manufacturers's
352 instructions. cDNA was synthesized from the purified RNA using the SuperScript[™] III First-Strand
353 Synthesis System (18080051; Invitrogen; Thermo Fisher Scientific, Inc.) with oligo (dT) by following the
354 manufacturer's protocol. The qRT-PCR reaction was performed using a final volume of 10 μ l includes 5 μ l
355 of PowerUp[™] SYBR[™] Green Master Mix 2x (Applied Biosystems, A25742), 1 μ M of each primer pair
356 (*serpine1* forward: GCCGTTAACTGTGTGGAAGA, *serpine1* reverse: ACGGTTAGTCTTCCTGAATGC;
357 *crhb* forward: CGTAACTGCCATCCAAGCG, *crhb* reverse: TCCCCGAGACATCCCAGTAT; *bcl2l1*
358 forward: CTCCTTCTCCACACACTCGA, *bcl2l1* reverse: GCGTGATGGATGAGGTGTTT; *psmb4* forward:
359 GGATGGTGTGTTGTTGACT, *psmb4* reverse: GTTCAAGGGTGGTGTGATCA; *ptgs2a* forward:
360 GATGAGTAGGGCTTCATGTTGA, *ptgs2a* reverse: CACCTGCAGTTCAAGGAGTC; β -*actin* forward:
361 ATGCAGAAGGAGATCACATCCC, β -*actin* reverse: GCTTGCTAATCCACATCTGCTG), 1 μ l of the cDNA
362 (10 ng in final concentration) and 2 μ l of UltraPure[™] DNase/RNase-Free Distilled Water dH₂O
363 (Invitrogen[™] Cat.#.: 10977015). The cycle threshold (Ct) value for the target genes was calculated using
364 QuantStudio[™] 3 real-time PCR system. Amplification conditions for qRT-PCR were as follows: 50 °C for
365 2 minutes, 95 °C for 10 minutes, followed by 40 cycles at 95 °C (15 seconds) and 60 °C (1 minute). Melting
366 curve was analyzed for each sample by following 95 °C for 15s, 60 °C for 1 minute and 95 °C for 1 second
367 after amplification reactions. Relative expression levels were calculated using $\Delta\Delta$ Ct method.

368 **Statistical analyses**

369 Pairwise comparisons were performed with unpaired parametric t test using GraphPad Prism v10.2.3.
370 ANOVA were performed to compare gene expression levels across ethanol concentration treatment
371 groups, with Dunnett's post-hoc comparisons.

372

373 **AUTHOR CONTRIBUTIONS**

374 Conceptualization, C.K., R.C.C., G.T.; methodology, C.K., N.N., E.Y.; formal analysis, C.K., N.N., E.Y.;
375 resources, C.K.; data curation, C.K., N.N., E.Y.; writing—original draft preparation, R.C.C., C.K., N.N., E.Y.;
376 writing—review and editing, R.C.C., C.K., N.N., G.T., E.Y.; funding acquisition, C.K.; All authors have read
377 and agreed to the published version of the manuscript.

378

379 **DISCLOSURES**

380 Authors declare no financial or competing interest.

381

182 REFERENCES

- 183 Abraira, V.E., and Ginty, D.D. (2013). The sensory neurons of touch. *Neuron* 79, 618-639.
184 10.1016/j.neuron.2013.07.051.
- 185 Achilleos, A., and Trainor, P.A. (2012). Neural crest stem cells: discovery, properties and potential for
186 therapy. *Cell Res* 22, 288-304. 10.1038/cr.2012.11.
- 187 ACOG (2011). Committee opinion no. 496: At-risk drinking and alcohol dependence: obstetric and
188 gynecologic implications. *Obstet Gynecol* 118, 383-388. 10.1097/AOG.0b013e31822c9906.
- 189 Adhish, M., and Manjubala, I. (2023). Effectiveness of zebrafish models in understanding human
190 diseases-A review of models. *Heliyon* 9, e14557. 10.1016/j.heliyon.2023.e14557.
- 191 Alsakran, A., and Kudoh, T. (2021). Zebrafish as a Model for Fetal Alcohol Spectrum Disorders. *Front*
192 *Pharmacol* 12, 721924. 10.3389/fphar.2021.721924.
- 193 Bruey, J.M., Bruey-Sedano, N., Luciano, F., Zhai, D., Balpai, R., Xu, C., Kress, C.L., Bailly-Maitre, B.,
194 Li, X., Osterman, A., et al. (2007). Bcl-2 and Bcl-XL regulate proinflammatory caspase-1 activation by
195 interaction with NALP1. *Cell* 129, 45-56. 10.1016/j.cell.2007.01.045.
- 196 Burden, M.J., Andrew, C., Saint-Amour, D., Meintjes, E.M., Molteno, C.D., Hoyme, H.E., Robinson,
197 L.K., Khaole, N., Nelson, C.A., Jacobson, J.L., and Jacobson, S.W. (2009). The effects of fetal alcohol
198 syndrome on response execution and inhibition: an event-related potential study. *Alcohol Clin Exp Res*
199 33, 1994-2004. 10.1111/j.1530-0277.2009.01038.x.
- 100 Burgess, H.A., and Burton, E.A. (2023). A Critical Review of Zebrafish Neurological Disease Models-1.
101 The Premise: Neuroanatomical, Cellular and Genetic Homology and Experimental Tractability. *Oxf Open*
102 *Neurosci* 2, kvac018. 10.1093/oons/kvac018.
- 103 Cadena, P.G., Cadena, M.R.S., Sarmah, S., and Marrs, J.A. (2020). Folic acid reduces the ethanol-induced
104 morphological and behavioral defects in embryonic and larval zebrafish (*Danio rerio*) as a model for fetal
105 alcohol spectrum disorder (FASD). *Reprod Toxicol* 96, 249-257. 10.1016/j.reprotox.2020.07.013.
- 106 Carter, R.C., Chen, J., Li, Q., Deyssenroth, M., Dodge, N.C., Wainwright, H.C., Molteno, C.D., Meintjes,
107 E.M., Jacobson, J.L., and Jacobson, S.W. (2018). Alcohol-related alterations in placental imprinted gene
108 expression in humans mediate effects of prenatal alcohol exposure on postnatal growth. *Alcohol Clin Exp*
109 *Res*.
- 110 Carter, R.C., Dodge, N.C., Molteno, C.D., Meintjes, E.M., Jacobson, J.L., and Jacobson, S.W. (2022).
111 Mediating and moderating effects of iron homeostasis alterations on fetal alcohol-related growth and
112 neurobehavioral deficits. *Nutrients* 14. 10.3390/nu14204432.
- 113 Carter, R.C., Jacobson, J.L., Molteno, C.D., Dodge, N.C., Meintjes, E.M., and Jacobson, S.W. (2016a).
114 Fetal alcohol growth restriction and cognitive impairment. *Pediatrics* 138, e20160775.
115 10.1542/peds.2016-0775.
- 116 Carter, R.C., Jacobson, J.L., Molteno, C.D., Jiang, H., Meintjes, E.M., Jacobson, S.W., and Duggan, C.
117 (2012). Effects of heavy prenatal alcohol exposure and iron deficiency anemia on child growth and body
118 composition through age 9 years. *Alcohol Clin Exp Res* 36, 1973-1982.
- 119 Carter, R.C., Jacobson, S.W., Molteno, C.D., Chiodo, L.M., Viljoen, D., and Jacobson, J.L. (2005).
120 Effects of prenatal alcohol exposure on infant visual acuity. *The Journal of Pediatrics* 147, 473-479.
121 10.1016/j.jpeds.2005.04.063.
- 122 Carter, R.C., Wainwright, H., Molteno, C.D., Georgieff, M.K., Dodge, N.C., Warton, F., Meintjes, E.M.,
123 Jacobson, J.L., and Jacobson, S.W. (2016b). Alcohol, methamphetamine, and marijuana exposure have
124 distinct effects on the human placenta. *Alc Clin Exp Res* 40, 753-764.
- 125 Deyssenroth, M.A., Williams, R.P., Lesseur, C., Jacobson, S.W., Jacobson, J.L., Cheng, H., Bose, P., Li,
126 Q., Wainwright, H., Meintjes, E.M., et al. (2024). Prenatal alcohol exposure is associated with changes in
127 placental gene co-expression networks. *Sci Rep* 14, 2687. 10.1038/s41598-024-52737-6.
- 128 Dlugos, C.A., and Rabin, R.A. (2007). Ocular deficits associated with alcohol exposure during zebrafish
129 development. *J Comp Neurol* 502, 497-506. 10.1002/cne.21320.

130 du Plessis, L., Jacobson, S.W., Molteno, C.D., Robertson, F.C., Peterson, B.S., Jacobson, J.L., and
131 Meintjes, E.M. (2015). Neural correlates of cerebellar-mediated timing during finger tapping in children
132 with fetal alcohol spectrum disorders. *Neuroimage Clin* 7, 562-570. 10.1016/j.nicl.2014.12.016.
133 Du, W., Chen, X., Shi, M., Bian, F., and Zhao, Z. (2020). Ethanol affects behavior and HPA axis activity
134 during development in zebrafish larvae. *Sci Rep* 10, 21402. 10.1038/s41598-020-78573-y.
135 Fan, J., Jacobson, S.W., Taylor, P.A., Molteno, C.D., Dodge, N.C., Stanton, M.E., Jacobson, J.L., and
136 Meintjes, E.M. (2016). White matter deficits mediate effects of prenatal alcohol exposure on cognitive
137 development in childhood. *Hum Brain Mapp* 37, 2943-2958. 10.1002/hbm.23218.
138 Fan, J., Taylor, P.A., Jacobson, S.W., Molteno, C.D., Gohel, S., Biswal, B.B., Jacobson, J.L., and
139 Meintjes, E.M. (2017). Localized reductions in resting-state functional connectivity in children with
140 prenatal alcohol exposure. *Hum Brain Mapp* 38, 5217-5233. 10.1002/hbm.23726.
141 Fernandes, Y., and Lovely, C.B. (2021). Zebrafish models of fetal alcohol spectrum disorders. *Genesis*
142 59, e23460. 10.1002/dvg.23460.
143 Fernandes, Y., Tran, S., Abraham, E., and Gerlai, R. (2014). Embryonic alcohol exposure impairs
144 associative learning performance in adult zebrafish. *Behav Brain Res* 265, 181-187.
145 10.1016/j.bbr.2014.02.035.
146 Fifer, W.P., Fingers, S.T., Youngman, M., Gomez-Gribben, E., and Myers, M.M. (2009). Effects of
147 alcohol and smoking during pregnancy on infant autonomic control. *Dev Psychobiol* 51, 234-242.
148 10.1002/dev.20366.
149 French, B.A., Dedes, J., Bardag-Gorce, F., Li, J., Wilson, L., Fu, P., Nan, L., and French, S.W. (2005).
150 Microarray analysis of gene expression in the liver during the urinary ethanol cycle in rats fed ethanol
151 intragastrically at a constant rate. *Exp Mol Pathol* 79, 87-94. 10.1016/j.yexmp.2005.06.006.
152 Gomez, D.A., May, P.A., Tabachnick, B.G., Hasken, J.M., Lyden, E.R., Kalberg, W.O., Hoyme, H.E.,
153 Manning, M.A., Adam, M.P., Robinson, L.K., et al. (2020). Ocular measurements in fetal alcohol
154 spectrum disorders. *Am J Med Genet A* 182, 2243-2252. 10.1002/ajmg.a.61759.
155 Graber, D.J., Costine, B.A., and Hickey, W.F. (2015). Early inflammatory mediator gene expression in
156 two models of traumatic brain injury: ex vivo cortical slice in mice and in vivo cortical impact in piglets. *J*
157 *Neuroinflammation* 12, 76. 10.1186/s12974-015-0298-4.
158 Hellems, K.G., Sliwowska, J.H., Verma, P., and Weinberg, J. (2010). Prenatal alcohol exposure: fetal
159 programming and later life vulnerability to stress, depression and anxiety disorders. *Neurosci Biobehav*
160 *Rev* 34, 791-807. 10.1016/j.neubiorev.2009.06.004.
161 Hoyme, H.E., Kalberg, W.O., Elliott, A.J., Blankenship, J., Buckley, D., Marais, A.-S., Manning, M.A.,
162 Robinson, L.K., Adam, M.P., Abdul-Rahman, O., et al. (2016). Updated clinical guidelines for diagnosing
163 fetal alcohol spectrum disorders. *Pediatrics* 138, e20154256. 10.1542/peds.2015-4256.
164 Hoyme, H.E., May, P.A., Kalberg, W.O., Kodituwakku, P., Gossage, J.P., Trujillo, P.M., Buckley, D.G.,
165 Miller, J.H., Aragon, A.S., Khaole, N., et al. (2005). A practical clinical approach to diagnosis of fetal
166 alcohol spectrum disorders: clarification of the 1996 Institute of Medicine criteria. *Pediatrics* 115, 39-47.
167 Jacobson, S.W. (1998). Specificity of neurobehavioral outcomes associated with prenatal alcohol
168 exposure. *Alcohol Clin Exp Res* 22, 313-320.
169 Jacobson, S.W., Hoyme, H.E., Carter, R.C., Dodge, N.C., Molteno, C.D., Meintjes, E.M., and Jacobson,
170 J.L. (2021). Evolution of the physical phenotype of fetal alcohol spectrum disorders from childhood
171 through adolescence. *Alcohol Clin Exp Res* 45, 395-408. 10.1111/acer.14534.
172 Jacobson, S.W., Jacobson, J.L., and Sokol, R.J. (1994). Effects of fetal alcohol exposure on infant
173 reaction time. *Alc Clin Exp Res* 18, 1125-1132.
174 Jacobson, S.W., Jacobson, J.L., Stanton, M.E., Meintjes, E.M., and Molteno, C.D. (2011). Biobehavioral
175 markers of adverse effect in fetal alcohol spectrum disorders. *Neuropsychol Rev* 21, 148-166.
176 10.1007/s11065-011-9169-7.
177 Jiang, H., Sun, Z., Zhu, X., Li, F., and Chen, Q. (2023). Essential genes *Ptgs2*, *Tlr4*, and *Ccr2* regulate
178 neuro-inflammation during the acute phase of cerebral ischemic in mice. *Sci Rep* 13, 13021.
179 10.1038/s41598-023-40255-w.

- i80 Kane, C.J.M., and Drew, P.D. (2021). Neuroinflammatory contribution of microglia and astrocytes in
i81 fetal alcohol spectrum disorders. *J Neurosci Res* 99, 1973-1985. 10.1002/jnr.24735.
- i82 Kimmel, C.B., Ballard, W.W., Kimmel, S.R., Ullmann, B., and Schilling, T.F. (1995). Stages of
i83 embryonic development of the zebrafish. *Dev Dyn* 203, 253-310. 10.1002/aja.1002030302.
- i84 Kimmel, C.B., Sepich, D.S., and Trevarrow, B. (1988). Development of segmentation in zebrafish.
i85 *Development* 104 Suppl, 197-207.
- i86 Koutsikou, S., Merrison-Hort, R., Buhl, E., Ferrario, A., Li, W.C., Borisjuk, R., Soffe, S.R., and Roberts,
i87 A. (2018). A simple decision to move in response to touch reveals basic sensory memory and mechanisms
i88 for variable response times. *J Physiol* 596, 6219-6233. 10.1113/JP276356.
- i89 Masehi-Lano, J.J., Deyssenroth, M., Jacobson, S.W., Jacobson, J.L., Molteno, C.D., Dodge, N.C.,
i90 Wainwright, H.C., Meintjes, E.M., Lesueur, C., Cheng, H., et al. (2023). Alterations in Placental
i91 Inflammation-Related Gene Expression Partially Mediate the Effects of Prenatal Alcohol Consumption on
i92 Maternal Iron Homeostasis. *Nutrients* 15. 10.3390/nu15194105.
- i93 May, P.A., Gossage, J.P., Kalberg, W.O., Robinson, L.K., Buckley, D., Manning, M., and Hoyme, H.E.
i94 (2009). Prevalence and epidemiologic characteristics of FASD from various research methods with an
i95 emphasis on recent in-school studies. *Dev Dis Res Rev* 15, 176-192. 10.1002/ddrr.68.
- i96 May, P.A., Marais, A.S., De Vries, M.M., Buckley, D., Kalberg, W.O., Hasken, J.M., Stegall, J.M.,
i97 Hedrick, D.M., Robinson, L.K., Manning, M.A., et al. (2021). The prevalence, child characteristics, and
i98 maternal risk factors for the continuum of fetal alcohol spectrum disorders: A sixth population-based
i99 study in the same South African community. *Drug Alcohol Depend* 218, 108408.
i00 10.1016/j.drugalcdep.2020.108408.
- i01 Muggli, E., Matthews, H., Penington, A., Claes, P., O'Leary, C., Forster, D., Donath, S., Anderson, P.J.,
i02 Lewis, S., Nagle, C., et al. (2017). Association Between Prenatal Alcohol Exposure and Craniofacial
i03 Shape of Children at 12 Months of Age. *JAMA Pediatr* 171, 771-780. 10.1001/jamapediatrics.2017.0778.
- i04 Neuhaus, S.C., Solnica-Krezel, L., Schier, A.F., Zwartkruis, F., Stemple, D.L., Malicki, J., Abdelilah, S.,
i05 Stainier, D.Y., and Driever, W. (1996). Mutations affecting craniofacial development in zebrafish.
i06 *Development* 123, 357-367. 10.1242/dev.123.1.357.
- i07 Oberlander, T.F., Jacobson, S.W., Weinberg, J., Grunau, R.E., Molteno, C.D., and Jacobson, J.L. (2010).
i08 Prenatal alcohol exposure alters biobehavioral reactivity to pain in newborns. *Alcoholism: Clinical and*
i09 *Experimental Research* 34, 681-692. 10.1111/j.1530-0277.2009.01137.x.
- i10 Pelisch, N., Dan, T., Ichimura, A., Sekiguchi, H., Vaughan, D.E., van Ypersele de Strihou, C., and
i11 Miyata, T. (2015). Plasminogen Activator Inhibitor-1 Antagonist TM5484 Attenuates Demyelination and
i12 Axonal Degeneration in a Mice Model of Multiple Sclerosis. *PLoS One* 10, e0124510.
i13 10.1371/journal.pone.0124510.
- i14 Pu, Z., Bao, X., Xia, S., Shao, P., and Xu, Y. (2022). Serpine1 Regulates Peripheral Neutrophil
i15 Recruitment and Acts as Potential Target in Ischemic Stroke. *J Inflamm Res* 15, 2649-2663.
i16 10.2147/JIR.S361072.
- i17 Qin, L., and Crews, F.T. (2012). NADPH oxidase and reactive oxygen species contribute to alcohol-
i18 induced microglial activation and neurodegeneration. *Journal of neuroinflammation* 9, 5. 10.1186/1742-
i19 2094-9-5.
- i20 Redza-Dutordoir, M., and Averill-Bates, D.A. (2016). Activation of apoptosis signalling pathways by
i21 reactive oxygen species. *Biochim Biophys Acta* 1863, 2977-2992. 10.1016/j.bbamcr.2016.09.012.
- i22 Ruffaner-Hanson, C., Noor, S., Sun, M.S., Solomon, E., Marquez, L.E., Rodriguez, D.E., Allan, A.M.,
i23 Caldwell, K.K., Bakhireva, L.N., and Milligan, E.D. (2022). The maternal-placental-fetal interface:
i24 Adaptations of the HPA axis and immune mediators following maternal stress and prenatal alcohol
i25 exposure. *Exp Neurol* 355, 114121. 10.1016/j.expneurol.2022.114121.
- i26 SAMHSA (2010). Results from the 2009 National Survey on Drug Use and Health. In SAMHSA, ed.
i27 (Health and Human Services).

- i28 Sarmah, S., Muralidharan, P., and Marrs, J.A. (2016). Embryonic Ethanol Exposure Dysregulates BMP
i29 and Notch Signaling, Leading to Persistent Atrio-Ventricular Valve Defects in Zebrafish. *PloS one* *11*,
i30 e0161205. 10.1371/journal.pone.0161205.
- i31 Serhan, C.N., Hong, S., Gronert, K., Colgan, S.P., Devchand, P.R., Mirick, G., and Moussignac, R.L.
i32 (2002). Resolvins: a family of bioactive products of omega-3 fatty acid transformation circuits initiated by
i33 aspirin treatment that counter proinflammation signals. *J Exp Med* *196*, 1025-1037.
i34 10.1084/jem.20020760.
- i35 Sidik, A., Dixon, G., Buckley, D.M., Kirby, H.G., Sun, S., and Eberhart, J.K. (2021). Exposure to ethanol
i36 leads to midfacial hypoplasia in a zebrafish model of FASD via indirect interactions with the Shh
i37 pathway. *BMC Biol* *19*, 134. 10.1186/s12915-021-01062-9.
- i38 Smith, S.M., Garic, A., Flentke, G.R., and Berres, M.E. (2014). Neural crest development in fetal alcohol
i39 syndrome. *Birth Defects Res C Embryo Today* *102*, 210-220. 10.1002/bdrc.21078.
- i40 Song, K., Kim, S., Na, J.Y., Park, J.H., Kim, J.K., Kim, J.H., and Kwon, J. (2014). Rutin attenuates
i41 ethanol-induced neurotoxicity in hippocampal neuronal cells by increasing aldehyde dehydrogenase 2.
i42 *Food Chem Toxicol* *72*, 228-233. 10.1016/j.fct.2014.07.028.
- i43 Stromland, K. (1987). Ocular involvement in the fetal alcohol syndrome. *Surv Ophthalmol* *31*, 277-284.
i44 10.1016/0039-6257(87)90028-2.
- i45 Suttie, M., Foroud, T., Wetherill, L., Jacobson, J.L., Molteno, C.D., Meintjes, E.M., Hoyme, H.E.,
i46 Khaole, N., Robinson, L.K., Riley, E.P., et al. (2013). Facial dysmorphism across the fetal alcohol
i47 spectrum. *Pediatrics* *131*, e779-788. 10.1542/peds.2012-1371.
- i48 Suttie, M., Wetherill, L., Jacobson, S.W., Jacobson, J.L., Hoyme, H.E., Sowell, E.R., Coles, C., Wozniak,
i49 J.R., Riley, E.P., Jones, K.L., et al. (2017). Facial Curvature Detects and Explicates Ethnic Differences in
i50 Effects of Prenatal Alcohol Exposure. *Alcohol Clin Exp Res* *41*, 1471-1483. 10.1111/acer.13429.
- i51 Terasaki, L.S., and Schwarz, J.M. (2017). Impact of Prenatal and Subsequent Adult Alcohol Exposure on
i52 Pro-Inflammatory Cytokine Expression in Brain Regions Necessary for Simple Recognition Memory.
i53 *Brain Sci* *7*. 10.3390/brainsci7100125.
- i54 Verhoeven, D., Schonenberg-Meinema, D., Ebstein, F., Papendorf, J.J., Baars, P.A., van Leeuwen,
i55 E.M.M., Jansen, M.H., Lankester, A.C., van der Burg, M., Florquin, S., et al. (2022). Hematopoietic stem
i56 cell transplantation in a patient with proteasome-associated autoinflammatory syndrome (PRAAS). *J*
i57 *Allergy Clin Immunol* *149*, 1120-1127 e1128. 10.1016/j.jaci.2021.07.039.
- i58 Wang, T., Lu, H., Li, D., and Huang, W. (2021). TGF-beta1-Mediated Activation of SERPINE1 is
i59 Involved in Hemin-Induced Apoptotic and Inflammatory Injury in HT22 Cells. *Neuropsychiatr Dis Treat*
i60 *17*, 423-433. 10.2147/NDT.S293772.
- i61 White, R.J., Collins, J.E., Sealy, I.M., Wali, N., Dooley, C.M., Digby, Z., Stemple, D.L., Murphy, D.N.,
i62 Billis, K., Hourlier, T., et al. (2017). A high-resolution mRNA expression time course of embryonic
i63 development in zebrafish. *Elife* *6*. 10.7554/eLife.30860.
- i64 Willford, J.A., Chandler, L.S., Goldschmidt, L., and Day, N.L. (2010). Effects of prenatal tobacco,
i65 alcohol and marijuana exposure on processing speed, visual-motor coordination, and interhemispheric
i66 transfer. *Neurotoxicol Teratol* *32*, 580-588. 10.1016/j.ntt.2010.06.004.
- i67 Williams, R.P., Lesseur, C., Cheng, H., Li, Q., Deyssenroth, M., Molteno, C.D., Meintjes, E.M.,
i68 Jacobson, S.W., Jacobson, J.L., Wainwright, H.C., et al. (2023). RNA-seq analysis reveals prenatal
i69 alcohol exposure is associated with placental inflammatory cells and gene expression. *Gene epub ahead*
i70 *of print* ([https://authors.elsevier.com/sd/article/S0378-1119\(23\)00792-8](https://authors.elsevier.com/sd/article/S0378-1119(23)00792-8)).
i71
i72

i73 **FIGURE LEGENDS**

i74 **Figure 1: Ethanol exposure causes phenotypic changes:** (A) Schematic view of the FASD model. (B) Exemplary
i75 phenotypic changes in zebrafish upon ethanol exposure. (C) Quantification of the sizes of eye, skull, ventrocranium,
i76 and heart chamber in control and 0.5% ethanol-treated groups. Scale bars equal 100 microns. $p < 0.001$: **, $p < 0.0001$:
i77 ****.

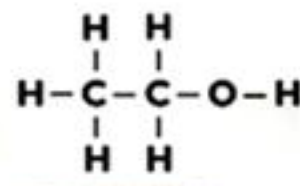
i78 **Figure 2: Ethanol exposure causes facial hypoplasia:** (A) Alcian blue staining of jaw cartilage. (B) Unpaired
i79 parametric t -test comparisons of jaw measurements. Scale bars equal 100 microns. $p < 0.0001$: ***, $p < 0.0001$: ****.

i80 **Figure 3: Ethanol exposure alters stimulus processing.** (A) Schematics for needle touch stimulus assay. (B)
i81 Representative images of recordings. Circles are start and end points after one round of tail touch. Scale bars
i82 equal 1 mm. (C) Quantification of burst swim distance and swimming speed of escape after stimulus (unpaired
i83 parametric t -test comparisons). Scale bars equal 1 mm.

i84 **Figure 4: Gene expression comparisons using quantitative real-time PCR for 5 genes differentially**
i85 **expressed based on prenatal alcohol exposure in human placentas.** Quantification graphs after different doses
i86 of alcohol exposure in zebrafish embryos. ANOVA and Dunnett's post-hoc test. $p < 0.032$: *, $p < 0.0021$: **, $p < 0.0002$:
i87 ***, $p < 0.0001$: ****.

AZebrafish
FASD model

0.5% ETOH

PHENOTYPE + BEHAVIOR +
GENE EXPRESSION ANALYSES

2-24 HOURS

POST FERTILIZATION

4.5 DAYS POST FERTILIZATION

**B**

Phenotypic outcomes



Ctrl

Reduced eye size



EtOH

Enlarged heart chamber
Gross body defects

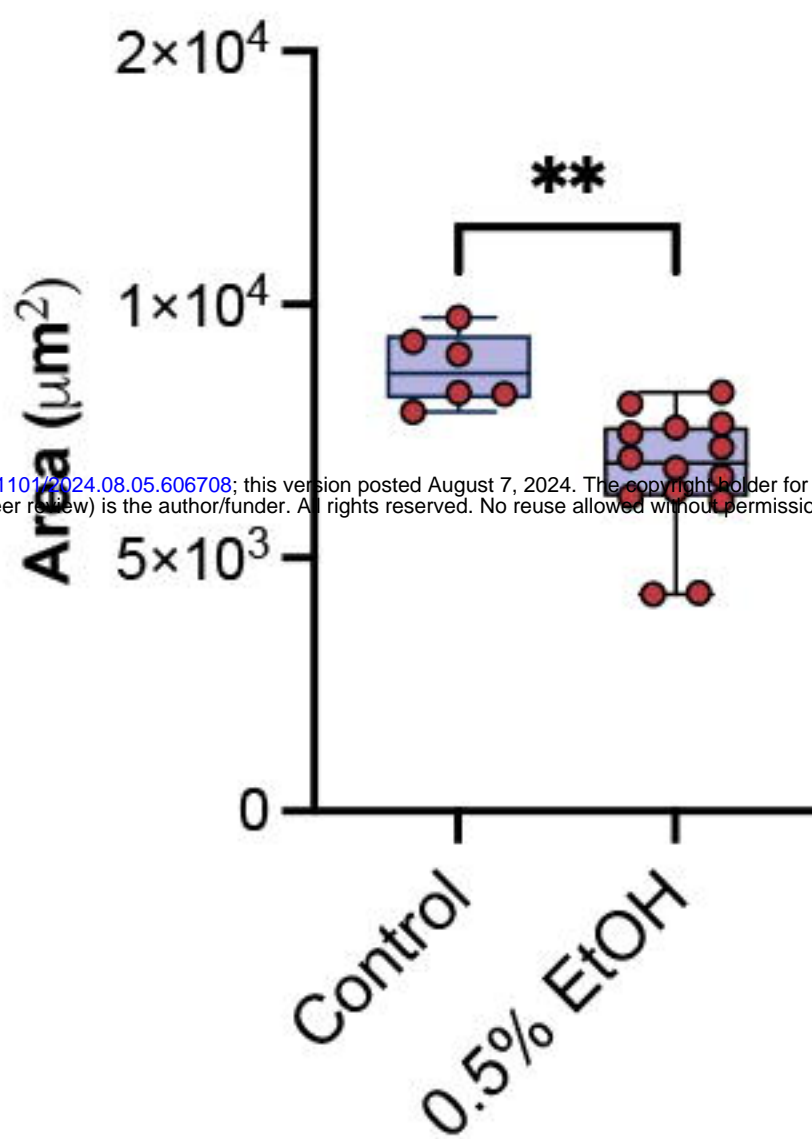
Ctrl

EtOH

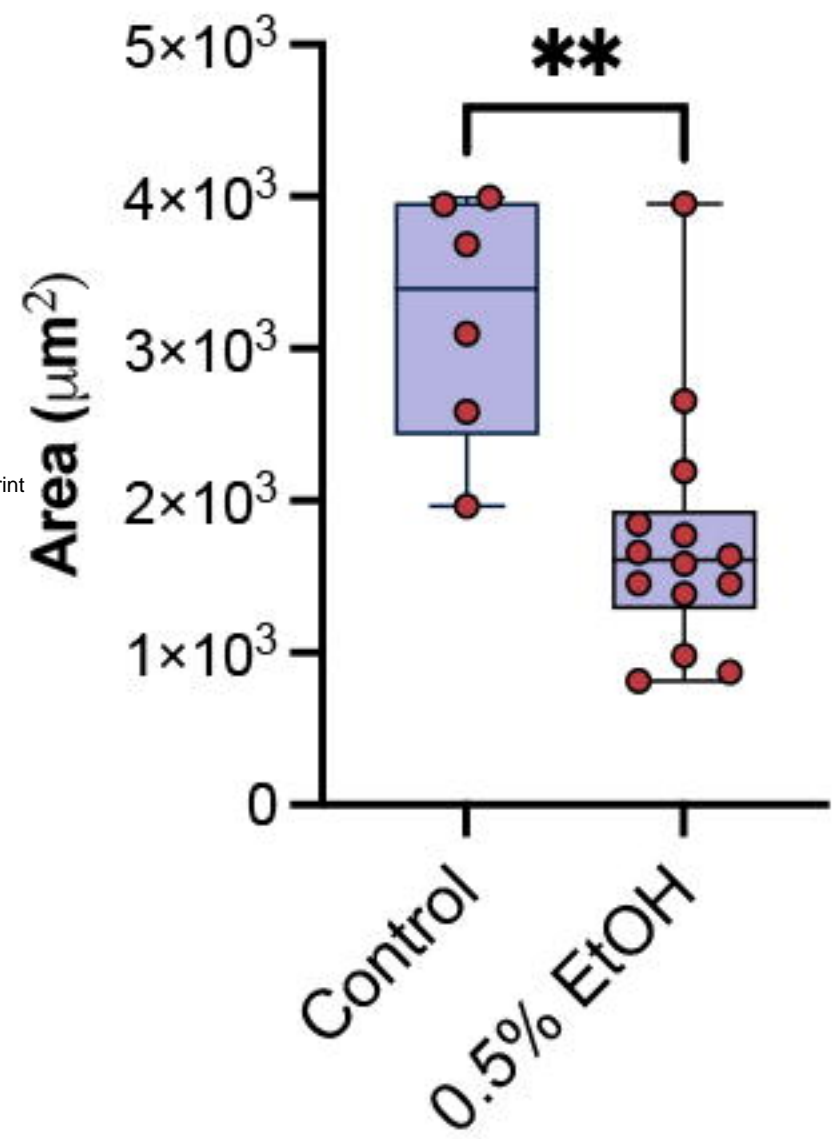
Diminished skull

Jaw malformations
Craniofacial defects**C**

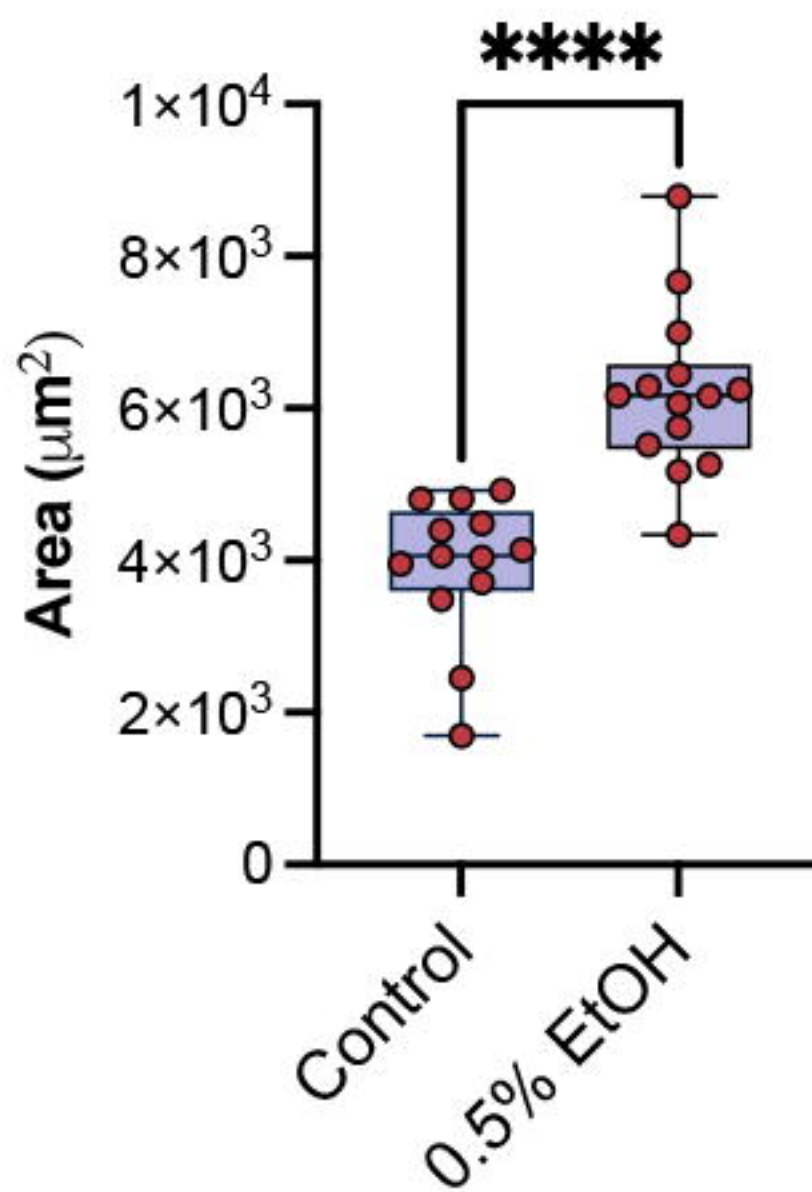
Eye size



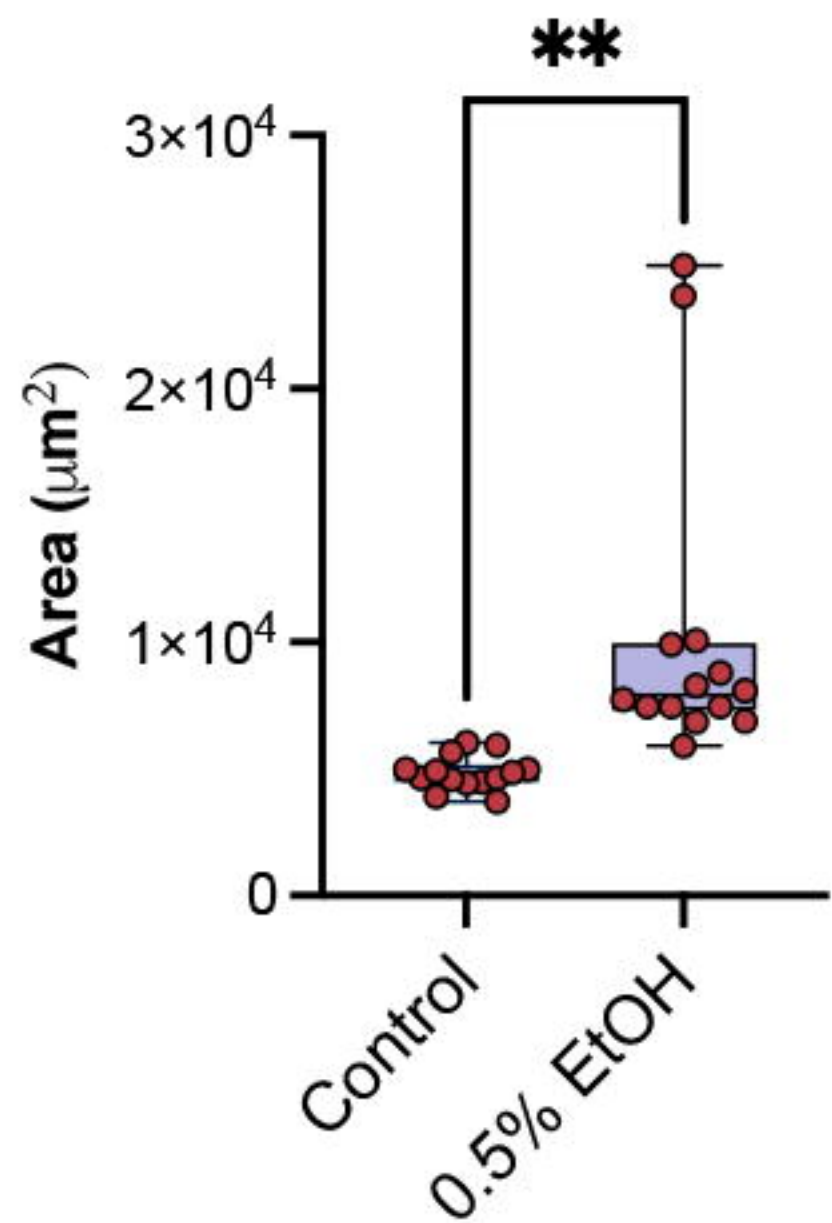
Skull size

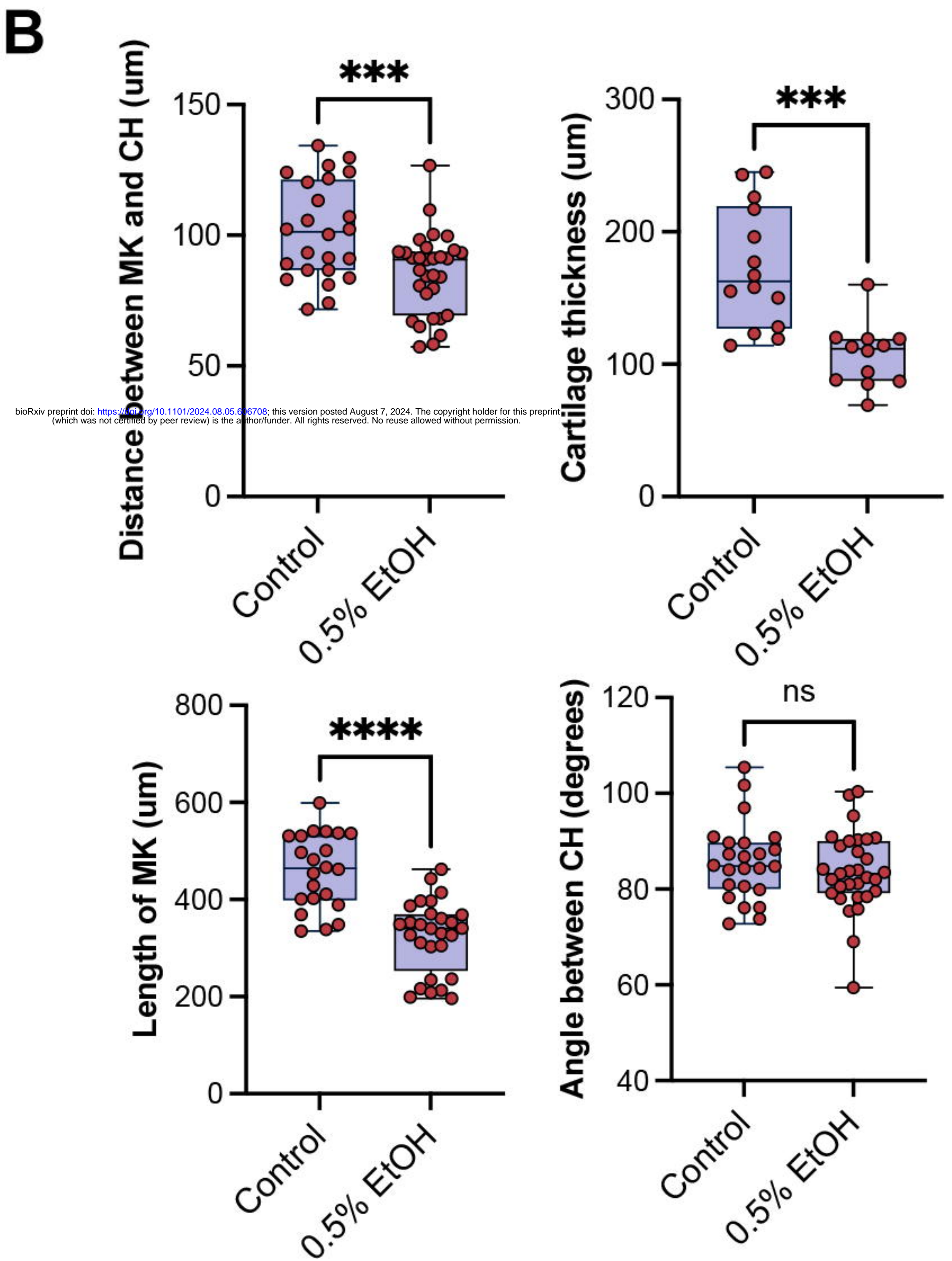
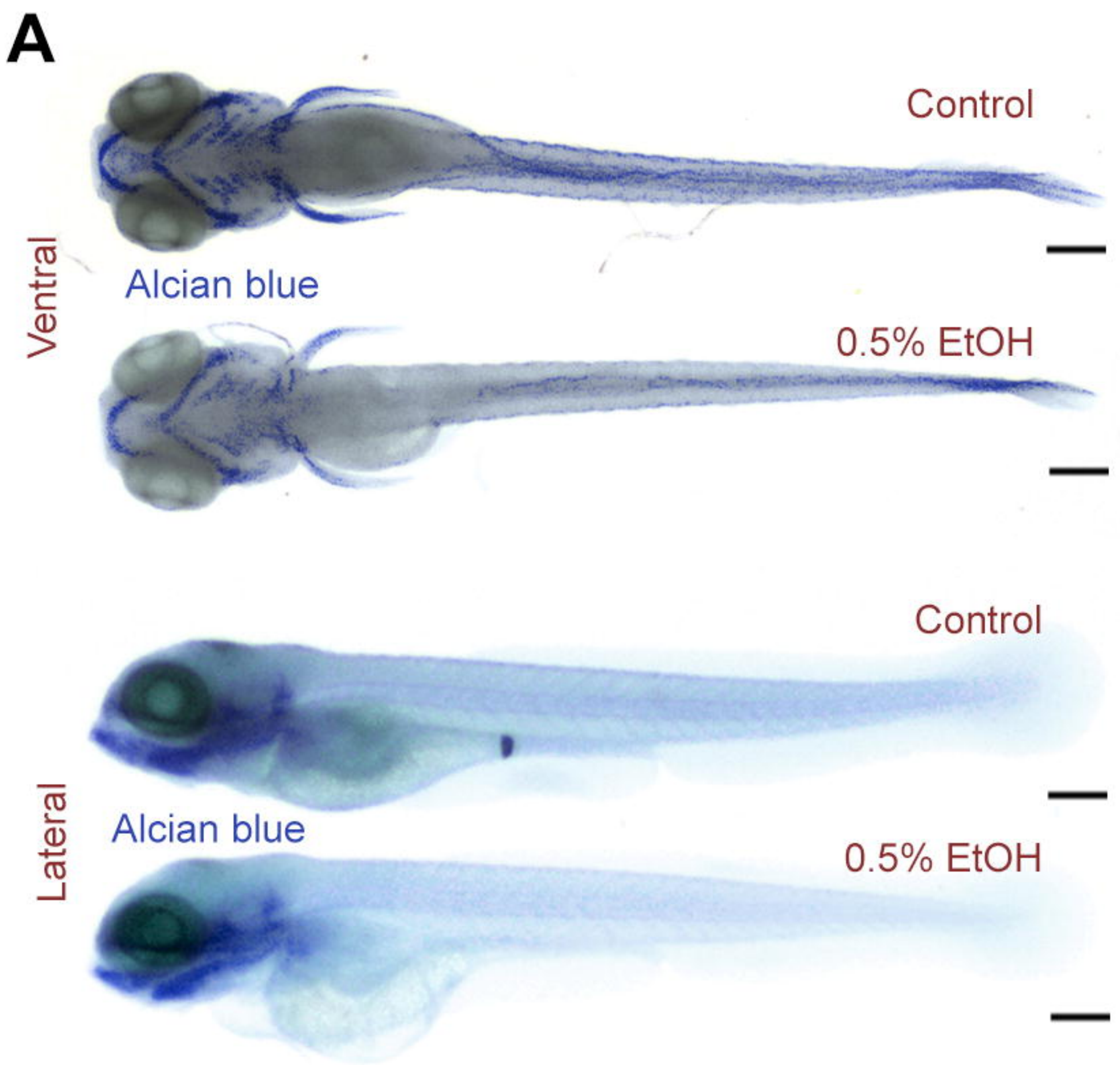


Ventricrocranium size



Heart chamber size





A Behavioral response

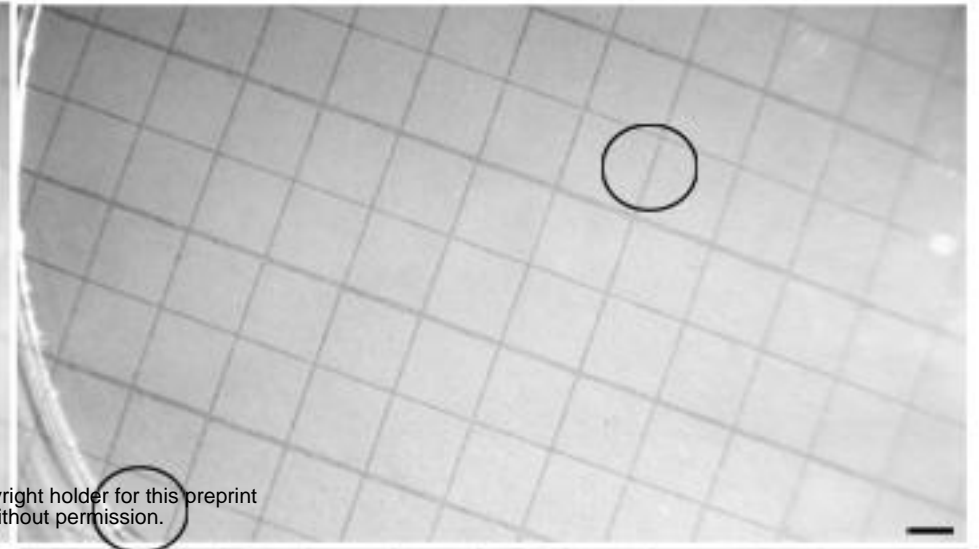
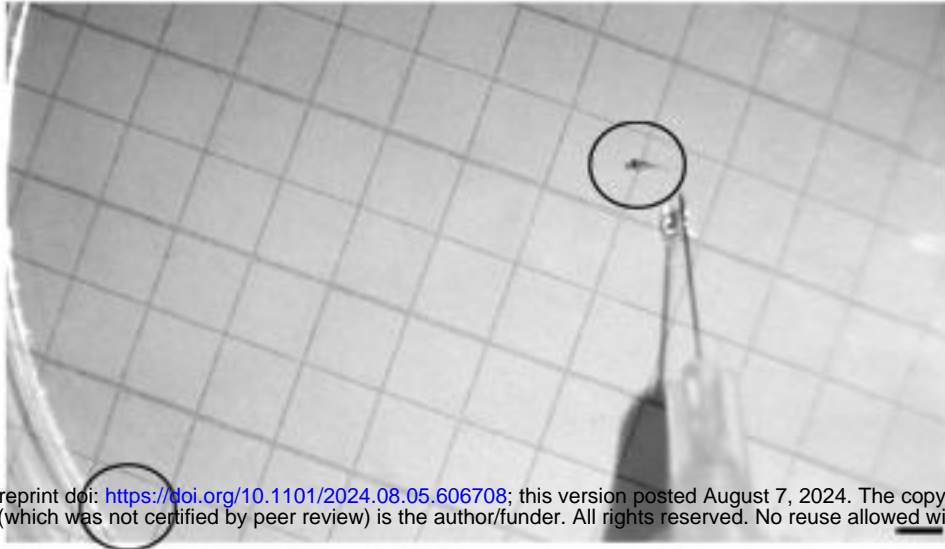


B

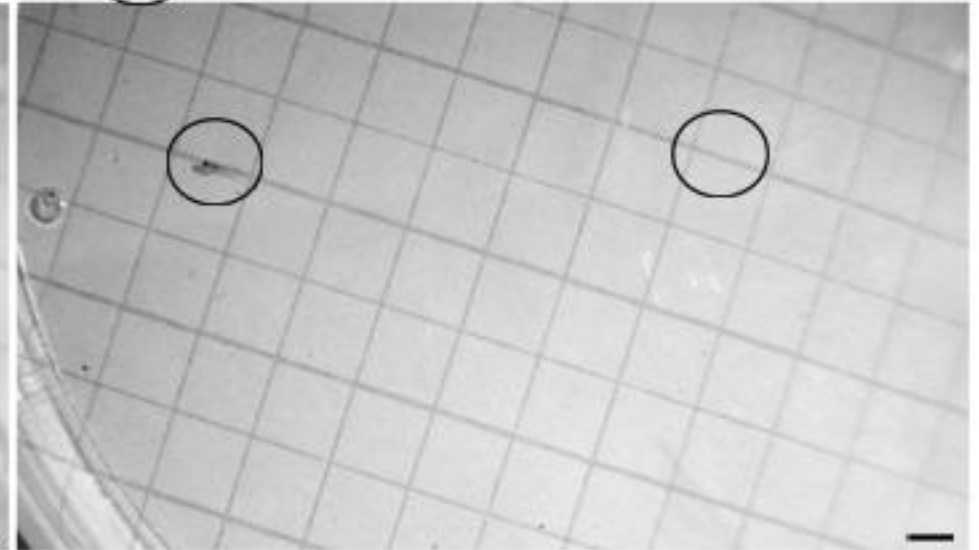
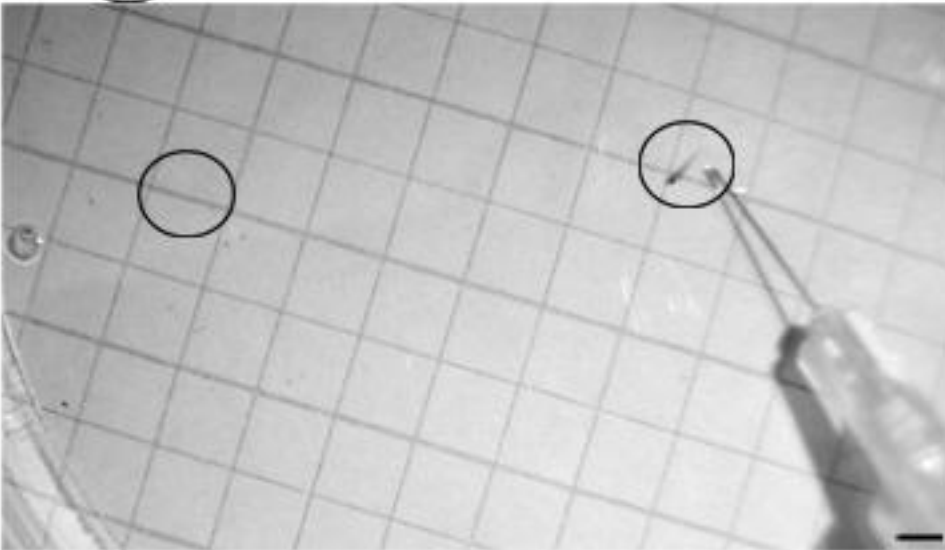
Before touch

After touch

Control



0.5% EtOH



C

